IASS 2018 BOSTON, JULY 16-20
CREATIVITY IN STRUCTURAL DESIGN

*Proceedings of the IASS Symposium 2018*
Creativity in Structural Design
July 16-20, 2018, MIT, Boston, USA
Caitlin Mueller, Sigrid Adriaenssens (eds.)

# Structural Optimization of Cross-Laminated Timber Panels

Paul Mayencourt*, Irina M. Rasid*, Caitlin Mueller*

*Massachusetts Institute of Technology
77 Massachusetts Avenue, 02139, Cambridge, MA, USA
mapaul@mit.edu

## Abstract

Cross-Laminated Timber (CLT) panels are gaining considerable attention in the United States as designers focus on building more ecological and sustainable cities. These panels can speed up construction on site due to their high degree of prefabrication, and consequently, CLT is deployed for slab systems, walls and composite systems in modern buildings. However, the structural use of the material is inefficient in CLT panels. The core of the material does not contribute to the structural behavior and acts merely as a spacer between the outer layers. This project offers an alternative design of an optimized CLT panel with the goal of reducing material consumption and increasing the efficiency of this building component, which can help it become more ubiquitous in building construction.

In this paper, a theoretical model for the behavior of optimized CLT panels is developed, and this model is compared with scaled physical load tests. The results demonstrate that the theoretical model accurately predicts physical behavior. Furthermore, around 20 % of material can be saved without major change in the structural behavior. The reduced material consumption and cost of the proposed optimized CLT panels can help mitigate the ecological impact of the construction industry, while offering a new competitive building product to the market.

**Keywords**: Cross-laminated Timber, Structural Optimization, Load Testing, Cellular Solids

## 1. Introduction

The building sector is responsible for 40-50% of the greenhouse gas emissions [1]. This contribution includes both the operational energy in buildings and the embodied energy in building materials and products. Two pathways have been extensively explored to reduce the ecological impact of building components: structural optimization and low embodied carbon building materials [2].

Structural optimization techniques aim to achieve similar or improved structural performance while reducing the cost of construction or material usage for a given structural condition. In 1638, Galileo Galilei first described a technique to shape structural beam following the moment diagram in order to reduce the amount of material needed to support a weight at the end of a cantilever [3]. Computation has since then expanded the potential of structural optimization with techniques like topology optimization to find minimal weight structural systems [4].

Within common construction materials, it is hard to define global low carbon building materials since their embodied energy depends on local technologies, availability of the resources, or even on the sustainability assessment itself. However, material selection charts [5] together with accurate data from Life Cycle Analysis (LCA) help designers walk through the decision process. A current study of the embodied energy of constructed buildings in More Economically Developed Countries shows that when considering environmental metrics at the building scale, construction made out of timber or masonry display a lower ecological impact on average [2]. Wood more specifically is appreciated for its carbon storage capabilities, especially when sourced from sustainably managed forests [6].

In the United State more specifically, timber construction is gaining interest with the construction of midrise timber buildings (T3, Minneapolis (Minnesota), Michael Green Architects, 2016; Framework Building, Portland (Oregon), Lever Architecture, in planning).

Cross-Laminated Timber (CLT) panels are particularly appreciated by the construction industry for their high potential of prefabrication, which speeds up construction on site and improves dimensional stability. Moreover, standard CLT panels can be used for two-way slabs as they can carry loads in both directions due to their cross lamination, and they can be used for walls as well. However, despite their clear advantages at present, the manufacturing of CLT panels could be made even more efficient. A recent benchmarking study by the Beck Group [7] revealed that 52% of the manufacturing cost of cross-laminated timber panels is the raw material, wood. This figure can go up to 77% in different studies [8]. Moreover, most current projects use CLT in one-way systems, which do not take full advantage of the mechanical properties achieved through cross-layer construction.

This project aims to structurally optimize CLT panels by selectively removing the cross-layer of the panels, which does not in theory contribute to the structural performance of the panels in many traditional applications. The initial idea is shown in Figure 1. Based on structural intuition, partially removing the core of the panel should not substantially influence its stiffness and strength, which are mostly controlled by the outer layers.

The first section of this paper describes the modeling of the optimized sandwich panels. Two different approaches were taken to model the modification of the cross-layer. The first approach is based on structural mechanics theory. The second model uses cellular material theory to model the core of the CLT panel, since the network of wood longitudinal and cross layer can be modeled as a square honeycomb core of a sandwich panel.

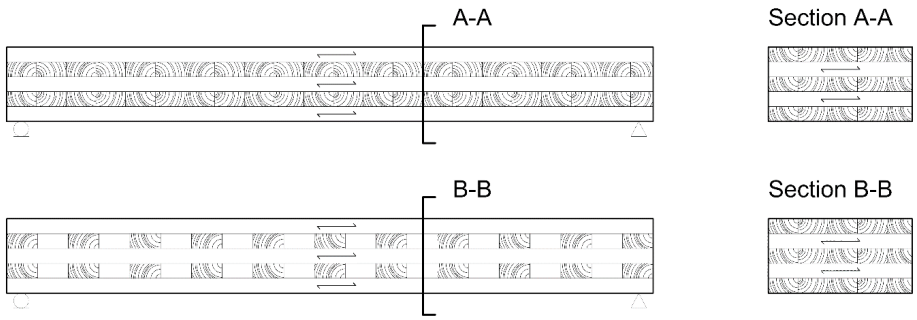


Figure 1: Optimized cross-laminated timber panels, the cross layer is selectively removed (in this case 50%) to reduce the material use.

The next section describes the fabrication and testing process for the six specimens used to validate the model, while also presenting the results of the load tests performed on each specimen.. The specimens correspond to a scaled version of an existing CLT product. The final part presents the results of the layout optimization of the panel layers, with the option of having different thicknesses for every layer. Finals thoughts, considerations for future work and conclusions are then discussed at the end of the paper.

## 2. Modeling

Two different models are used to describe the behavior of the optimized panel. Based on the theory of sandwich panels and cellular solids materials theory [9], the first strategy models the core of the panel as a square honeycomb structure and the outer layer as a wood skin. The second model is based on the theory of structural mechanics—it describes the change in section properties with an updated moment of inertia.

### 2.1. Cellular solids model

Cellular solids and sandwich panel's theory offer methods for optimizing the structural behavior of CLT panels, which is the objective of this study. Sandwich panel's theory separates the behavior of the core of the panel and the behavior of the panel's skin. In this analogy, the core of the panel is represented as a rectangular honeycomb (Figure 2).

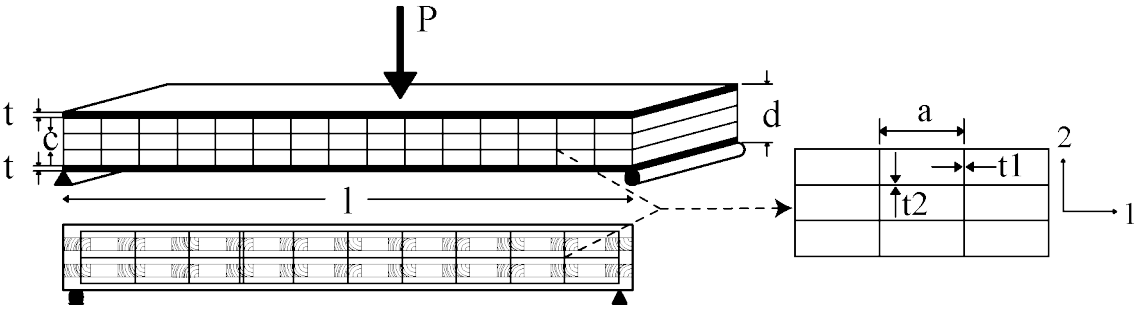


Figure 2: Cross-laminated timber panels analyzed as a sandwich panel with a core modeled as rectangular honeycomb solid and the outer wood layers as the sandwich panel's skin.

The properties of the core in directions 1 and 2 are then analogous to the in-plane properties ($E_1$*, $G_{12}$*) of a rectangular honeycomb.

The in-plane properties of a rectangular honeycomb with dimensions a, b, $t_1$ and $t_2$ as defined in Figure 2 are derived in [10]. For rectangular honeycombs, the relative density is: $\frac{\rho^*}{\rho_s} = \frac{at_2+bt_1}{ab}$. This is an approximation, which applies if $a \gg t_1$ and $b \gg t_2$. This assumption clearly does not hold for CLT, as this would result in relative densities that are greater than 1, which has no physical meaning. However, since $b=2t_2$, the equation can be rewritten, resulting in the equation shown in Figure 3.

| | |
|---|---|
| Relative density | $\frac{\rho_c^*}{\rho_s} = \frac{a+t_1}{2a}$ |
| Young's modulus | $E_1^* = \frac{t_1}{a} E_{S,parallel}$ |
| Shear modulus | $G_{12}^* = \frac{t_1^3 t_2^3}{2at_2(at_1^3 + 2t_2^4)} E_{s,perpendicular}$ |
| Weight | $W = \rho_c^* gwlxt_2;$ |

where:

| | | | |
|---|---|---|---|
| w: | the width of the layer | $\rho^*_c$: | the density of the panel |
| l: | the span of the panel | x: | the number of plies |

Figure 3: Set of equations to describe in-plane properties of core rectangular honeycomb.

The compliance of the CLT panel under three point bending with central load P is then given by its bending and shear contribution [9]:

$$\frac{\delta}{P} = \frac{l^3}{B_1(EI)_{eq}} + \frac{l}{B_2(AG)_{eq}}$$

Taking $(EI)_{eq} = \frac{E_f btd^2}{2}$ and $(AG)_{eq} = wcG_{12}^*$ , the compliance can then be approximated as,

$$\frac{\delta}{P} = \frac{2l^3}{B_1 E_f w\, {}^{t_2}/_2\, (xt_2)^2} + \frac{l}{B_2 wxt_2 G_{12}^*}$$

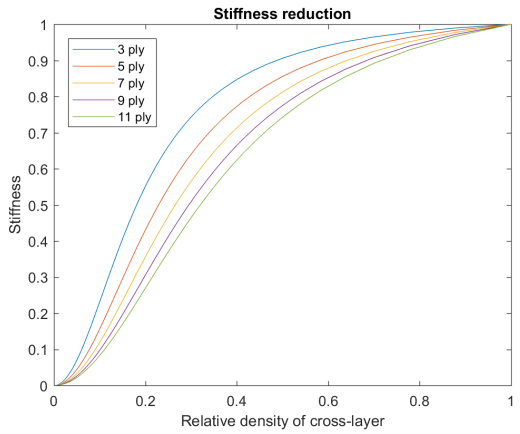


Figure 4 Stiffness against relative density of the cross-layer based on the rectangular honeycomb model.

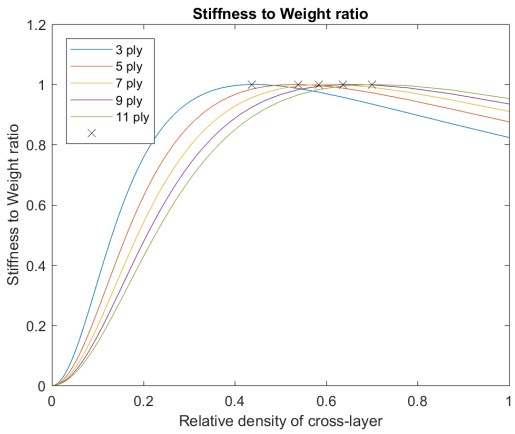


Figure 5 Stiffness to weight ratio against relative density of the cross-layer based on the rectangular honeycomb model.

The results from the bending stiffness calculations, summarized in Table 1, provide the optimum relative density of the cross-layer to maximize the stiffness of the CLT, while keeping the weight of the panel to a minimum.

Table 1: Optimal relative densities for different panel compositions

| 3 ply | 5 ply | 7 ply | 9 ply | 11 ply |
|---|---|---|---|---|
| 0.44 | 0.53 | 0.58 | 0.63 | 0.70 |

## 2.2. Structural mechanics model

In this second model, the structural behavior of CLT panels is based on the US CLT Handbook [11] and on the design guide for CLT after the Eurocode 5 [12]. The stiffness of the panel is derived from a combination of the shear stiffness (mainly influenced by the cross layer) and the bending stiffness, which takes the biggest contribution from the longitudinal layers. The same model is used to derive the stiffness and strength of the optimized panels. The relative density $\rho^*/\rho_s$ of the core is introduced into the equation as a modifier of the contribution of each layer. In this case, only the cross layer get its relative density modified (even layer numbers). A relative density of 1 corresponds to a standard CLT panels with complete cross-layers.

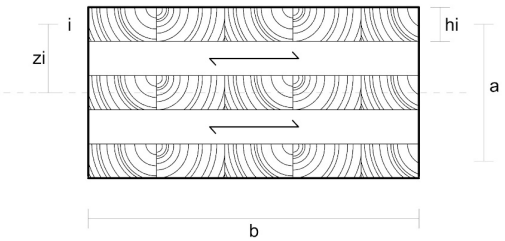


For simplification of the notation, we have:

$$\left(\frac{\rho^*}{\rho_s}\right)_i = \begin{cases} 0 \; if \; i \; unven \\ \left(\frac{\rho^*}{\rho_s}\right) \; if \; i \; even \end{cases}$$

Effective Bending stiffness

$$EI_{ef} = \sum_{i=1}^{n} \left(\frac{\rho^*}{\rho_s}\right)_i E_i b_i \cdot \frac{h_i^3}{12} + \sum_{i=1}^{n} \left(\frac{\rho^*}{\rho_s}\right)_i E_i A_i z_i^2$$

Effective shear stiffness

$$GA_{eff} = \frac{a^2}{\left[\left(\frac{h_1}{2G_1 b_1}\right) + \left(\sum_{i=2}^{n-1} \frac{h_i}{G_i b_i}\left(\frac{\rho^*}{\rho_s}\right)_i\right) + \left(\frac{h_n}{2G_n b_n}\right)\right]}$$

Apparent bending stiffness

$$EI_{app} = \frac{EI_{eff}}{1 + \frac{K_s EI_{eff}}{GA_{eff} L^2}}$$

Bending strength $$F_b S_{eff} = F_b \frac{2EI_{eff}}{E_1 h}$$

Shear strength $$F_s \left(\frac{Ib}{Q_{eff}}\right) = \left(\frac{\rho^*}{\rho_s}\right) F_s \frac{EI_{eff}}{\sum_{i=1}^{n/2} E_i h_i z_i \left(\frac{\rho^*}{\rho_s}\right)_i}$$

Normalized weight $$w = \frac{\left(\frac{(\#ply - 1)\left(\frac{\rho^*}{\rho_s}\right)}{2} + \frac{\#ply + 1}{2}\right)}{\#ply}$$

where:

$b_i$: the width of the layer

$E_i$: the stiffness of the layer

$h_i$: the thickness of the layer

$z_i$: the distance from the neutral axis to the center of the layer

$A_i$: the area of the layer

a: the distance between the center of the two extreme layers

$G_i$: the rolling shear stiffness of the layer

$K_s$: constant representing the loading and fixities conditions (14.4 in the case of simply supported beam)

$F_b$: the allowable bending stress

$E_1$: the stiffness parallel to the grain:

$F_S$: the allowable rolling shear stress

Figure 6 CLT section and parameters

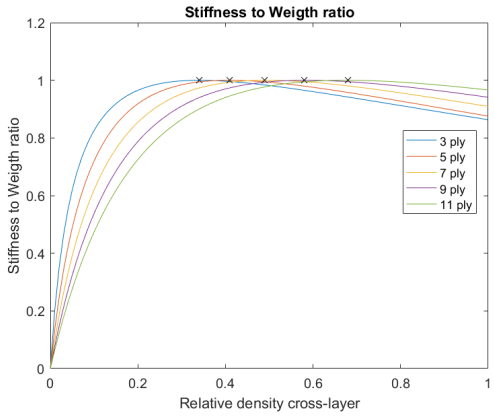


Figure 7: Stiffness to Weight ratio as a function of the relative density of the cross-layer.

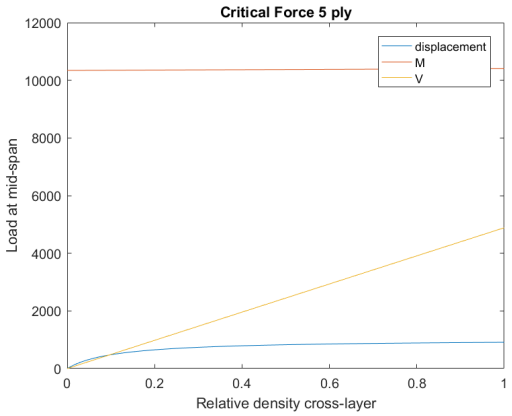


Figure 8: Critical force design for different panel compositions as a function of the relative density. The panel are limited by the deflection limit.

While the shear strength decreases with the removal of the core, it can be shown that the deflection will always be the governing criteria in CLT design. Figure 8 plots the force that corresponds to the limiting criteria for every relative density of the core. The blue curve (for the displacement limit, here defined as L/360) is always located below the shear criteria (V) and the bending resistance (M). Results for different CLT thicknesses and plies show a similar outcome. The next table (Table 2) gives the optimal strength to weight ratio results for the structural mechanics model.

Table 2: Optimal relative densities for different panel compositions

| 3 ply | 5 ply | 7 ply | 9 ply | 11 ply |
|---|---|---|---|---|
| 0.34 | 0.41 | 0.49 | 0.58 | 0.68 |

## 2.2. Comparison between models

It is apparent that the two models gives results that generally agree. Both models predict an optimal stiffness to weight ratio for relative core density of the cross-layer lower than one. The models also

predict two different regions, a plateau (around the optimal relative density of the core) followed by a sharp drop. Beyond a basic agreement of the trends, however, the predictions of the optimum relative density of the core layers are different, with the structural mechanics model showing a peak at 0.41 while the cellular solids model gives a peak at 0.53 for the 5 ply panel.

A key limitation of the cellular solids model is the definition of the vertical cell wall elasticity of the rectangular honeycomb core. In the honeycomb model, the vertical cell walls are deformed in bending. In CLT panels, the cross-layer is mainly deformed in rolling shear. This was only partly captured by defining the cell walls with different modulus of elasticity. Finally, the theory of cellular solids also assumes a small cell size relative to the size of the honeycomb, which is not true in this case. While the both models agree qualitatively, the structural mechanics model was judged to be more accurate, and thus forms the basis for the following sections of the paper.

### 2.2. Physical load testing

In order to control the prediction of the theoretical model, a series of scaled down CLT panels were constructed and load tested. The specimens were loaded in three point bending test for a span of 1.1m, and have a cross section of 30 mm by 60 mm. Each layer has a height of 6mm. The panels were fabrication on campus by the author with 38.1 mm by 139.7 mm boards of Select Structural grade of Douglas Fir-Larch, the highest visual structural grade with characteristic material properties published by the National Design Specification [14]. However, the material characteristics cannot be used directly to predict the strength of the scaled down panels because of the scale of the wood elements (6 mm by 12 mm). Since the load testing aims to compare changes in structural stiffness between two panels, the material properties for this scale were not characterized for the scope of this paper. A wood glue Titebond III [15] was used for the lamination of the panels.

The physical load testing results are provided in Figure 8. These results show that the reduction of stiffness and weight are comparable to the ones predicted by the models. The specimen are a scaled down version of existing panel manufactured in North America (Nordic Structures [13], 175-5s). Two types of 5-ply panels were tested: a standard CLT panel and an optimized panel with a core density of the cross layers of 0.5. Three specimens of each types were load tested to failure.

The optimized panels are 21.8 % lighter than the standard panels for a 7% reduction of stiffness (13.8% if the outliers are considered). However, the optimized panels also have a load capacity 31.2% lower. The standard and optimized panels also displayed different failure modes—the standard panels experienced a face rupture of the wood on the tension side of the panels, and the optimized panels failed by delamination of rupture of the bond at the cross layer interface.

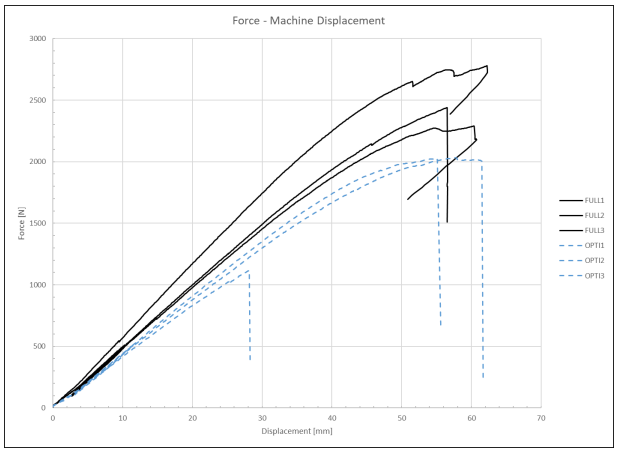


Figure 9: Test result for the six specimens

The poor glue bonding between the layers due to an uneven contact surface can explain the delamination failure in the case of the optimized panels. The effect of the poor glue bond was especially obvious when the cross layer showed no sign of wood rupture but rather of the bond between the layers. The poor glue

bond is not as critical for the standard panels due to the redundancy of the cross layer. Nevertheless, these tests make it clear that if optimized CLT panels are to be effective in building applications, they must be carefully constructed to ensure failure is controlled by the material properties rather than issues of quality. It is assumed that the manufactured quality of prefabricated panels could be considerably higher than prototypes developed by the authors.

Following the analysis and load testing of the behavior of CLT panels with core variable density, these models are used to run a layout optimization of CLT panels.

## 2.2. Layout Optimization

### *2.1.1. Problem definition*

This section presents the results of the layout optimization for the CLT panel build-up. Currently, most of CLT panels are built with constant layer heights. However, this paper presents the following optimization problem, in which the panels can be built with layers of different heights, and the cross layer can have a relative densities lower than one:

$$\begin{aligned} \text{minimize} \quad & Volume \\ \text{subject to} \quad & EI_{app} \geq \alpha EI_{app,initial} \\ & L \leq L_{crit} = \frac{1}{12.05} \frac{EI^{0.293}}{\rho A^{0.122}} \\ & h_1 \geq d_{fire} \end{aligned}$$

A simplified procedure is used for the control of the vibrations and fire safety. The vibration limit is compared to a critical span, defined in [11] by the stiffness, the mass of the panels and a structural system parameter. For fire safety, a simplified char design is used. In this case, the depth of the outer layers have to be larger than the required char depth, which is set as a constraint for the optimization. The initial layer thickness is set to 34.9 mm.

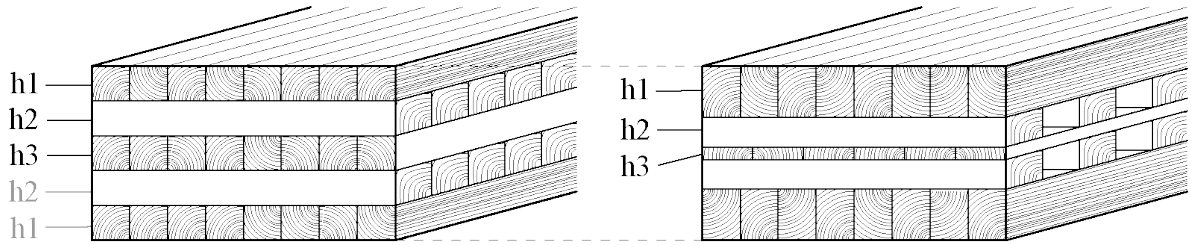


Figure 10: Result of the layout optimization for cross-laminated timber. For the same structural depth and stiffness, the panel layout on the right is 18% lighter.

The optimization was solved using *fmincon* in Matlab [16]. The parameter α was set to 99%, the bounds for the layer thicknesses for h1, h2 and h3 to [12.7 mm, 88.9 mm]. The layer thicknesses of the optimal panel are $h_1$=51.22 mm, $h_2$=29.72 mm and $h_3$=12.7 mm. Figure 10 shows the new panel layout that achieves the same stiffness but is 18% less material intensive.

## 2.2. Conclusions and future work

This research demonstrates that a slight modification of the layout of a standard CLT panel could reduce its material consumption by 18% without any loss of performance. The new layout reduces the shear capacity of the panel, but the shear is not the limiting design criteria. In cases where the displacement limit does not govern the design, greater material savings can be achieved.

Full-scale prototypes are required to assess the constructability of the optimized layout and its structural performance. Digital fabrication can be implemented to enable a mass-customization of the panel for each specific application. However, manufacturers have to find a reasonable balance between the advantages of standardized products and a customized panel that has to go through the code approval process.

Future work will extend the range of panel layout and confirm their structural performance with load tests. Furthermore, the void in the panel could be used for service lines or as a possible cavity for lateral reinforcement in composites two-way systems.

Building CLT panels with layers of different heights will require a slight modification of the supply chain for manufacturer. In fact, in the US, CLT panels are manufactured from dimensional lumber widely available. This change would be easier to adopt for a vertically integrated manufacturer that has a greater control on the milling process and pricing or would require requesting custom milled lumber. As shown in the first part of the paper, material price in CLT manufacturing is responsible for 52% of the total price, translated in a price saving of 9% to 13%, without any changes of the structural quality of the products.

Reducing the material consumption and using low embodied carbon materials in buildings is key to mitigating the impact of the building sector on the environment. Ubiquitous building elements such as CLT panels offer a tremendous opportunity to have an impact at scale. The cost competitiveness and performance of the optimized CLT panels presented in this paper can contribute to a greater adoption of massive timber elements in buildings.

## Acknowledgements

We thank Stephen Rudolph, Andrew Brose and Demi Fang for assistance with the load tests, and Nathan Brown and Lorna Gibson for comments on the material of this paper.

## Remark

The content of this work is protected by U.S. provisional patent. Please contact the author if would like more information.

## References

[1] U.S. Energy Information Administration, “Use of Energy in the United States - Energy Explained, Your Guide To Understanding Energy - Energy Information Administration.” [Online]. Available: https://www.eia.gov/energyexplained/index.cfm?page=us_energy_use. [Accessed: 23-Jan-2018].
[2] C. (Catherine E. L. De Wolf, “Low carbon pathways for structural design : embodied life cycle impacts of building structures,” Thesis, Massachusetts Institute of Technology, 2017.
[3] S. P. Timoshenko, “History of Strength of Materials,” 1983. [Online]. Available: http://store.doverpublications.com/0486611876.html. [Accessed: 23-Jan-2018].
[4] W. R. Spillers and K. M. MacBain, *Structural Optimization*. Springer US, 2009.
[5] M. F. Ashby, *Materials Selection in Mechanical Design*. Butterworth-Heinemann, 2016.
[6] U. Dangel, *Turning Point in Timber Construction: A New Economy*, 1. edition. Basel: Birkhauser, 2016.
[7] The Beck Group, “California Assessment of Wood Business Innovation Opportunities and Markets, Phase 2 Report,” 2015.
[8] B. Toosi, “Cross Laminated Timber - The Market Opportunities in North America,” 2011.
[9] L. J. Gibson and M. F. Ashby, *Cellular Solids: Structure and Properties*. Cambridge University Press, 1999.
[10] A. M. Hayes, A. Wang, B. M. Dempsey, and D. L. McDowell, “Mechanics of linear cellular alloys,” *Mech. Mater.*, vol. 36, no. 8, pp. 691–713, Aug. 2004.
[11] E. Karacabeyli and B. Douglas, *US CLT Handbook*. FPInnovations, 2013.
[12] M. Wallner-Novak, J. Koppelhuber, and K. Pock, *Brettsperrholz Bemessung: Grundlagen für Statik und Konstruktion nach Eurocode : Informationen für die Berechnung und konstruktive Gestaltung von Holztragwerken*. Wien: ProHolz Austria, 2013.
[13] Nordic Engineered Wood, “Nordic X-Lam - Nordic Engineered Wood, Non-residential Design, Construction Guide.” 2015.
[14] American Wood Council, *National Design Specification 2018 - Supplement - Design Values for Wood Construction*. American Wood Council, 2017.

[15] Titebond, "Titebond III: Ultimate Wood Glue." [Online]. Available: http://www.titebond.com/titebond_wood_glues/Ultimate_Wood_Glue.aspx. [Accessed: 24-Jan-2018].
[16] The MathWorks, *MATLAB: "Matlab 2016b."* 2016.